Evidence for Luttinger-Liquid Behavior in Crossed Metallic Single-Wall Nanotubes

B. Gao,[1] A. Komnik,[2] R. Egger,[3] D. C. Glattli,[1,4] and A. Bachtold[1]

[1]*Laboratoire Pierre Aigrain, Ecole Normale Supérieure, 75231 Paris 05, France*
[2]*Physikalisches Institut, Albert-Ludwigs-Universität, 79104 Freiburg, Germany*
[3]*Institut für Theoretische Physik, Heinrich-Heine-Universität, 40225 Düsseldorf, Germany*
[4]*SPEC, CEA Saclay, 91191 Gif-sur-Yvette, France*

(Received 28 November 2003; published 27 May 2004)

Transport measurements through crossed metallic single-wall nanotubes are presented. We observe a zero-bias anomaly in one tube which is suppressed by a current flowing through the other nanotube. These results are compared with a Luttinger-liquid model which takes into account electrostatic tube-tube coupling together with crossing-induced backscattering processes. Explicit solution of a simplified model is able to describe qualitatively the observed experimental data with only one adjustable parameter.

DOI: 10.1103/PhysRevLett.92.216804 PACS numbers: 73.63.Fg, 73.23.–b, 73.40.Gk, 73.50.Fq

Single-wall carbon nanotubes (SWNTs) continue to receive a lot of attention in connection with electronic transport in interacting one-dimensional (1D) quantum wires. Metallic SWNTs represent a nearly perfect 1D system, with μm-long mean free paths [1–3] and only two spin-degenerate transport channels, where it has been theoretically predicted that electrons form a (four-channel) Luttinger-liquid (LL) rather than a conventional Fermi liquid phase [4,5]. Experimental evidence for LL behavior in an individual SWNT has been reported in tunneling [6–8] and resonant tunneling measurements [9], revealing a pronounced suppression in the tunneling density of states [zero-bias anomaly (ZBA)]. Although the observed power-law ZBA can be consistently explained by the LL theory, it is difficult to rule out alternative explanations based on, e.g., environmental dynamical Coulomb blockade. Furthermore, a very similar ZBA has been experimentally observed in multiwall nanotubes [10–12] although such systems are known to be disordered multichannel wires [13,14]. It is therefore of importance to find LL signatures beyond the ZBA for tunneling into individual SWNTs [6–8]. Following the proposal of Refs. [15,16], in this Letter we report experimental evidence suggesting a LL picture from electrical transport through two crossed metal SWNTs.

Albeit crossed nanotubes have been investigated by other groups before [17–19], so far no transport measurements for crossed metallic SWNTs have been reported below 300 K. In our experiments, the conductance is measured first in one tube with the other left floating. The conductance decreases as the temperature or the bias is reduced, in a way very similar to that of tunneling experiments in SWNTs. Interestingly, the ZBA disappears as the current is increased through the second tube. Below we discuss the relationship between these results and LL predictions. The electrostatic coupling between charges moving in different tubes pins the sliding low-energy excitations (plasmons). When current is imposed to flow, the generated potential fluctuations suppress the pinning in the other tube, thus enhancing its conductance. Explicit calculations based on LL theory reproduce the measurements rather well.

The laser-ablation grown SWNTs are dispersed from a suspension in dichloroethane onto an oxidized Si wafer. Atomic-force microscopy (AFM) is then used to locate crossed SWNTs with an apparent height of ≈ 1 nm, presumably corresponding to individual SWNTs. Next, Cr/Au electrodes are attached using electron-beam lithography. An example of a device is shown in Fig. 1(a). The separation L between the crossing and the electrodes is chosen to be $\simeq 300$ nm. For shorter L, undesired finite-size effects may come into play, while for much longer L, the probability is enhanced to find disorder centers along the SWNTs that complicate the analysis. Devices were then studied above 20 K, where the thermal length $L_T = \hbar v_F/kT$, with Fermi velocity v_F, remains short compared to L. More than 60 samples have been fabricated, but we have never been lucky enough to achieve a device with two crossed metal SWNTs and, at the same time, to keep all contact resistances low, so that Coulomb blockade is negligible. Four times an almost ideal device has been obtained, where only one of the four contact resistances was large. Measurements have been carried out on these four devices, which all gave similar results. A representative set of measurements on one device is presented next. In this device, at $T = 220$ K, the two-point

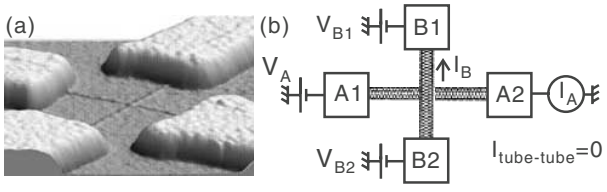

FIG. 1. (a) AFM image of a crossed SWNT junction. The electrode height is 45 nm. (b) Scheme of the device together with the measurement setup. The AFM image cannot discriminate which tube lies on top of the other.

resistances at zero bias of the two SWNTs (henceforth called A and B) are $R_A = 19\ \mathrm{k}\Omega$ and $R_B = 524\ \mathrm{k}\Omega$, while the four-point resistance of the tube-tube junction is $R_X = 277\ \mathrm{k}\Omega$. Other two-point measurements with electrode $B1$ contacted, see Fig. 1(b) for the electrode identification, give also large resistance, suggesting that the large R_B comes from a poor interface between tube B and electrode $B1$. Note that the two-point measurements are achieved with the other electrodes left floating. When T is decreased, this large contact resistance induces Coulomb blockade (CB) oscillations in tube B with zero current for different regions in the backgate voltage V_g. In the following, V_g is fixed at a broad CB peak.

The device is further characterized by measuring the LL interaction parameter g [4,5] from the tunneling density of states. Figure 2 shows the differential tube-tube tunneling conductance $G_X(V_X, T) = dI_X/dV_X$ measured in a four-point configuration. Electrons tunnel from the middle of one SWNT to the middle of the second SWNT (bulk-bulk tunneling). The double-logarithmic plots of $G_X(V_X, T)$ in Fig. 2 are described by a power-law scaling with slope $\alpha_{\text{bulk-bulk}} \simeq 1.1$. Using $\alpha_{\text{bulk-bulk}} = (g^{-1} + g - 2)/4$ [4,5], we find $g \simeq 0.16$. This is somewhat lower than reported values $g \simeq 0.2$ for tunneling into a SWNT from a metal electrode [6–8], reflecting slightly stronger Coulomb interactions among the electrons. This is presumably due to different geometries in Refs. [6–8] and in our device, in particular, concerning the electrode location reponsible for screening effects.

Figure 3(a) shows the differential conductance dI_A/dV_A measured on tube A as a function of V_A for different T and with tube B left floating. A clear ZBA is observed, which becomes larger as T is decreased. Such a ZBA has been observed many times in SWNTs [6–8] and implies that a barrier lies along the tube or at the interface with the electrodes. Figure 3(b) shows $dI_A/dV_A(V_A)$ when a current I_B is imposed to flow through the second tube. Interestingly, the ZBA is progressively suppressed when I_B is increased. We note that the ZBA suppression depends only on the intensity of I_B and not on its sign. For these measurements, the sample was biased such that no current flows from tube A to tube B through the junction. To achieve this, first a three-point measurement is carried out on tube A under bias V_A to determine the potential V_A^X at the crossing. The voltage drops between the crossing and each electrode are recorded as a function of V_A and are found to be equal. In a second step, the three-point measurement is carried out on tube B to record V_B^X at the crossing as a function of V_B. This time, the voltage drops are very different on both sides of the tube reflecting the large contact resistance at the $B1$ electrode. Finally, I_A is measured as a function of V_A for different V_B where voltages V_{B1} and V_{B2} applied on electrodes $B1$ and $B2$ are continually adjusted so that $V_A^X = V_B^X$; see Fig. 1(b). Since most of V_B drops at the bad contact $B1$, we give instead of V_B the current I_B in the Fig. 3(b) legend, which is measured while tube A is left floating.

We review now some possible explanations for the I_B dependence of the ZBA. Let us first consider the effect of joule heating. Note that heating effects are generally disregarded in tunneling experiments into individual

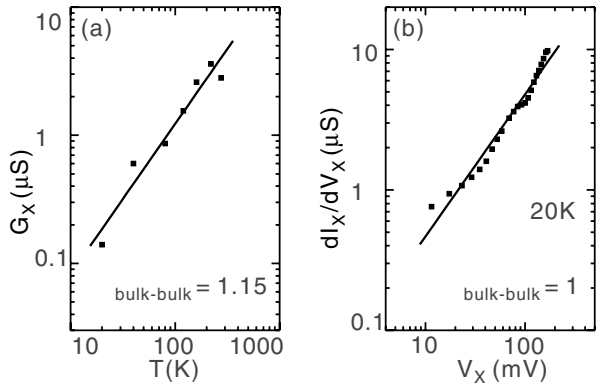

FIG. 2. Tunneling measurement on the tube-tube junction in a four-probe configuration. (a) Linear conductance $G_X(V_X = 0, T)$. (b) Differential conductance $dI_X/dV_X(V_X, T = 20\ \mathrm{K})$.

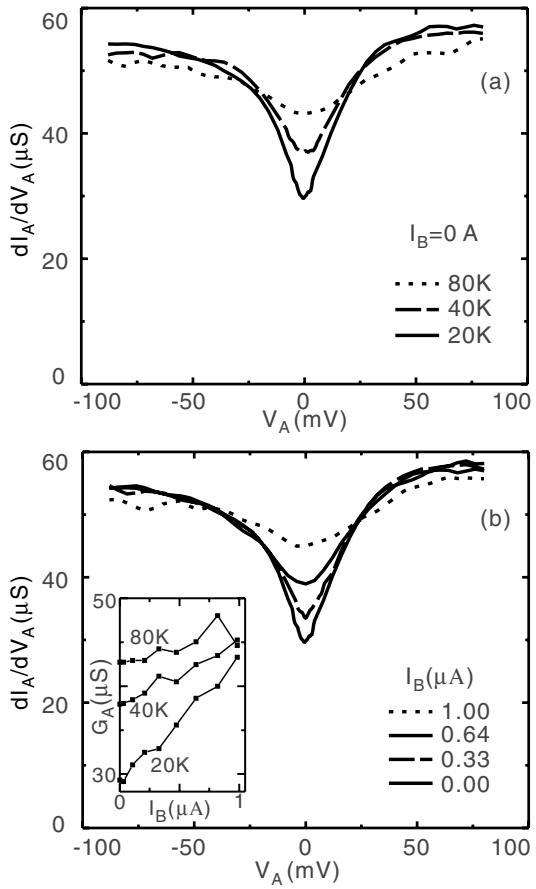

FIG. 3. Differential conductance $dI_A/dV_A(V_A)$ measured on SWNT A (a) for different T and (b) for different I_B through SWNT B at 20 K. The inset in (b) shows G_A for $V_A = 0$ as a function of I_B. $I_B = 1\ \mu$A corresponds to $V_B = 0.8$ V. The other points are separated in bias by $\Delta V_B = 0.1$ V.

tubes [6–8,10–12]. However, the poor $B1$ contact releases significant heat in tube B. Part of it flows through tube A, which may then change the temperature sensitive G_A. Unfortunately, the temperature rise ΔT is difficult to estimate, already because little is known about the thermal conductances of individual SWNTs and tube-tube junctions. Nevertheless, a qualitative statement can be made. Since $G_A(20\ \mathrm{K}, 0.6\ \mu\mathrm{A}) \simeq G_A(40\ \mathrm{K}, 0\ \mathrm{A})$ and $G_A(40\ \mathrm{K}, 0.6\ \mu\mathrm{A}) \simeq G_A(80\ \mathrm{K}, 0\ \mathrm{A})$, the same heat input 360 nW would give rise to temperature increases $20 \rightarrow 40$ K and $40 \rightarrow 80$ K. This would imply that the thermal conductance decreases with T, which is very unlikely in this T range [20–22]. Hence thermal effects alone cannot explain our observations. Another explanation might be related to the capacitive coupling between tubes. The conductance can vary with V_g as in interference experiments [2,3]. Here G_A is indeed observed to fluctuate with V_g. One could thus argue that tube B just acts as a gate. However, the fluctuations with V_g, which are lower than 2.1 μS at 20 K and above, cannot account for the large modulation of $G_A(I_B)$. We conclude that another explanation is needed to account for our results.

Next we compare the data to LL predictions for two crossed SWNTs with identical LL parameter g [15,16]. Since the experiment is carried out at zero tube-tube current, single-electron tunneling at the crossing can be neglected, and hence only tube-tube electrostatic coupling and crossing-induced backscattering (CIB) processes need to be taken into account. The importance of CIB processes due to the tube deformation has been stressed in several previous experimental [19,23] and theoretical studies [24,25]. Both are taken as local couplings acting only at the crossing. Adopting the bosonization formalism [26], for $g < 1/5$, the most relevant part of the density operator in tube $\alpha = A, B$ is $\rho_\alpha(x) \propto \cos[\sqrt{16\pi g}\varphi_{c+,\alpha}(x)]$, where $\varphi_{c+,\alpha}$ is the plasmon field for the total charge sector; see Eq. (6.10) in Ref. [27]. Choosing spatial coordinates such that $x = 0$ corresponds to the crossing, the Hamiltonian $H = H_0 + H_{\mathrm{AB}} + H_{\mathrm{CIB}}$ consists of the clean LL part, $H_0 = \sum_\alpha H_{\mathrm{LL},\alpha}$, a local tube-tube coupling $H_{\mathrm{AB}} = \lambda_0 \rho_A(0)\rho_B(0)$, and the CIB part $H_{\mathrm{CIB}} = \lambda_1 \rho_A(0) + \lambda_2 \rho_B(0)$. Standard renormalization group (RG) analysis [26] yields the lowest-order flow equations

$$\frac{d\lambda_0}{d\ell} = (1-8g)\lambda_0 + 2\lambda_1\lambda_2, \quad \frac{d\lambda_{1,2}}{d\ell} = (1-4g)\lambda_{1,2}. \quad (1)$$

The initial coupling constants $\lambda_{0,1,2}(0)$ could be accessed from microscopic considerations but here are only assumed to be nonzero. Integration of Eq. (1) yields $\lambda_{1,2}(\ell) = \lambda_{1,2}(0)\exp[(1-4g)\ell]$ and

$$\lambda_0(\ell) = [\lambda_0(0) - 2\lambda_1(0)\lambda_2(0)]e^{(1-8g)\ell} + 2\lambda_1(0)\lambda_2(0)e^{(2-8g)\ell}. \quad (2)$$

Apparently, at low energies (large ℓ), the RG flow is completely dominated by $\lambda_0(\ell)$ due to the last term in Eq. (2). Keeping only the λ_0 term, the neutral channels decouple, and one arrives at the single-channel model of Refs. [15,16], taken at effective interaction parameter $K_{\mathrm{eff}} = 4g - 1/2$. Taking $g = 0.16$, this gives $K_{\mathrm{eff}} = 0.14$. For this argument, it is crucial that $g < 1/5$ and $\lambda_{1,2}(0) \neq 0$, for otherwise no ZBA occurs for any $g > 1/8$. The CIB processes therefore drive the electrostatic tube-tube coupling λ_0 to be the dominant interaction in this crossed geometry. The strong coupling λ_0 then generates a ZBA which disappears when current flows in the second tube, in agreement with experiments. For $K_{\mathrm{eff}} = 1/4$, this can be made explicit by a simple analytical solution of the resulting transport problem [16]. This corresponds to $g = 0.1875$, close to our experimental value $g = 0.16$. While the exact solution can be obtained for any K_{eff} as well [28], away from $K_{\mathrm{eff}} = 1/4$ this solution is less transparent and shows only slight differences. For $K_{\mathrm{eff}} = 1/4$, the current through SWNTs $\alpha = A, B$ is

$$I_\alpha = \frac{4e^2}{h}[V_\alpha - (U_+ \pm U_-)/\sqrt{2}], \quad (3)$$

with $U_\pm$ obeying the self-consistency relations

$$eU_\pm = 2kT_B \mathrm{Im}\Psi\left(\frac{1}{2} + \frac{kT_B + i(eV_\pm - eU_\pm)}{2\pi kT}\right), \quad (4)$$

with the digamma function Ψ, $V_\pm = (V_A \pm V_B)/\sqrt{2}$, and an effective coupling strength T_B, which depends on the system parameters, in particular, on the initial couplings $\lambda_{0,1,2}(0)$. The solution (3) and (4) employs radiative boundary conditions [28], which in turn assume ideal tube-electrode contacts. This assumption is, however, overly restrictive here since $L_T \ll L$ (see above). For our device, where three contacts are nearly ideal and only one has low transparency, Eqs. (3) and (4) then receive only small corrections, see Sec. 4 in Ref. [16].

Figures 4(a) and 4(b) show modified $dI_A/dV_A(V_A)$ curves of Fig. 3. Indeed, Fig. 3 shows that the high-bias differential conductance dI_A/dV_A saturates at $(17.9\ \mathrm{k}\Omega)^{-1}$ instead of $4e^2/h$, which is the high-bias conductance predicted by Eqs. (3) and (4). We therefore argue that a resistance $R_c = 11.4\ \mathrm{k}\Omega$ lies in series with the I_B dependent contribution of the intertube coupling in order to obtain this dI_A/dV_A saturation. R_c, presumably located at the tube-electrode interfaces, is taken constant. This approximation is quite good since the ZBA tends to disappear for large I_B, leaving only a weak $1/R_c$ conductance modulation; see Fig. 3(b). Moreover, the conductance is known to change only slightly with T or V in experiments on individual SWNTs that are well contacted with contact resistance of the order $10\ \mathrm{k}\Omega$ [2,3]. Figures 4(c) and 4(d) show the predicted $dI_A/dV_A(V_A)$ curves calculated from Eq. (3) with (4). The effective coupling T_B is set at $T_B = 11.6$ K to get agreement with the experimental value for G_A at 20 K; $I_B = 0$ and $V_A = 0$. After fixing T_B, no parameter is tuned to calculate the

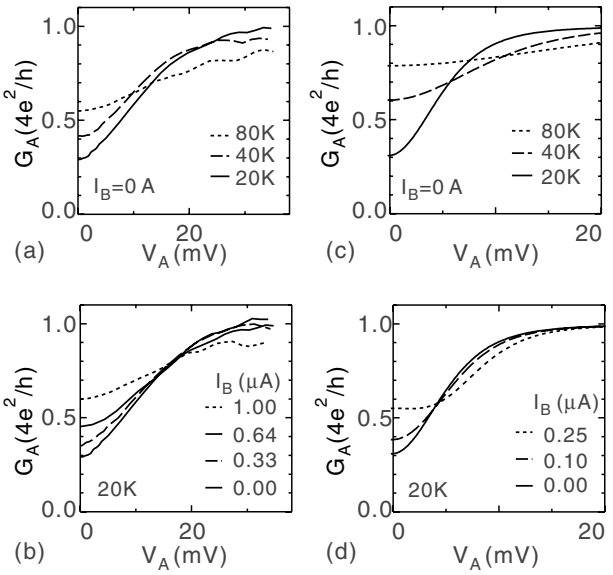

FIG. 4. Differential conductance $dI_A/dV_A(V_A)$ symmetrized and modified from Fig. 3 for (a) different T and (b) for different I_B. Theoretical predictions for two interacting SWNTs are shown in (c) and (d). The curves in (d) are obtained for constant biases V_B. The corresponding currents I_B, which are calculated with Eqs. (3) and (4) for $V_A = 0$, are given in the legend.

conductance variation with V_A, T, and I_B. Despite the above-mentioned approximations, the agreement of theory and experiment is quite good. We note in passing that Eqs. (3) and (4) predict the emergence of minima in $dI_A/dV_A(V_A)$ for $I_B \gtrsim 1\ \mu$A, which have not been observed though. One probable cause could be the inelastic scattering on optical phonons taking place at such large currents [29], which are not included in Eqs. (3) and (4).

In conclusion, we have observed on a crossed SWNT junction a ZBA in one tube which is suppressed by a current flowing through the other. These measurements are in rather good agreement with an analysis based on LL theory, which predicts a barrier along each tube generated by the electrostatic tube-tube interaction and controlled by current in the other tube. The crossed tube junction thus provides an interesting system offering external control of the barrier transmission in a LL that will be useful, e.g., in noise measurements.

We thank B. Plaçais, J. M. Berroir, N. Regnault, B. Trauzettel, and C. Delalande for discussions and R. Smalley for the SWNTs. LPA is CNRS-UMR8551 associated to Paris 6 and 7. This research has been supported by ACN and sesame programs, by the EU network DIENOW, by the DFG-SFB TR 12, and by the Landesstiftung Baden–Württemberg.

[1] A. Bachtold, M. S. Fuhrer, S. Plyasunov, M. Forero, E. H. Anderson, A. Zettl, and P. L. McEuen, Phys. Rev. Lett. **84**, 6082 (2000).
[2] J. Kong, E. Yenilmez, T. W. Tombler, W. Kim, H. Dai, R. B. Laughlin, L. Liu, C. S. Jayanthi, and S. Y. Wu, Phys. Rev. Lett. **87**, 106801 (2001).
[3] W. Liang, M. Bockrath, D. Bozovic, J. H. Hafner, M. Tinkham, and H. Park, Nature (London) **411**, 665 (2001).
[4] R. Egger and A. O. Gogolin, Phys. Rev. Lett. **79**, 5082 (1997).
[5] C. Kane, L. Balents, and M. P. A. Fisher, Phys. Rev. Lett. **79**, 5086 (1997).
[6] M. Bockrath, D. H. Cobden, J. Lu, A. G. Rinzler, R. E. Smalley, L. Balents, and P. L. McEuen, Nature (London) **397**, 598 (1999).
[7] Z. Yao, H. W. Ch. Postma, L. Balents, and C. Dekker, Nature (London) **402**, 273 (1999).
[8] H. W. C. Postma, M. de Jonge, Z. Yao, and C. Dekker, Phys. Rev. B **62**, R10 653 (2000).
[9] H. W. Ch. Postma, T. Teepen, Z. Yao, M. Grifoni, and C. Dekker, Science **293**, 76 (2001).
[10] A. Bachtold, M. de Jonge, K. Grove-Rasmussen, P. L. McEuen, M. Buitelaar, and C. Schönenberger, Phys. Rev. Lett. **87**, 166801 (2001).
[11] R. Tarkiainen, M. Ahlskog, J. Penttilä, L. Roschier, P. Hakonen, M. Paalanen, and E. Sonin, Phys. Rev. B **64**, 195412 (2001).
[12] W. Yi, L. Lu, H. Hu, Z. W. Pan, and S. S. Xie, Phys. Rev. Lett. **91**, 076801 (2003).
[13] R. Egger and A. O. Gogolin, Phys. Rev. Lett. **87**, 066401 (2001).
[14] E. G. Mishchenko, A. V. Andreev, and L. I. Glazman, Phys. Rev. Lett. **87**, 246801 (2001),
[15] A. Komnik and R. Egger, Phys. Rev. Lett. **80**, 2881 (1998).
[16] A. Komnik and R. Egger, Eur. Phys. J. B **19**, 271 (2000).
[17] M. S. Fuhrer, J. Nygard, L. Shih, M. Forero, Y. G. Yoon, M. S. C. Mazzoni, H. J. Choi, J. Ihm, S. G. Louie, A. Zettl, and P. L. McEuen, Science **288**, 494 (2000).
[18] J. Kim, K. Kang, J.-O. Lee, K.-H. Yoo, J.-R. Kim, J. W. Park, H. M. So, and J.-J. Kim, J. Phys. Soc. Jpn. **70**, 1464 (2001).
[19] J. W. Janssen, S. G. Lemay, L. P. Kouwenhoven, and C. Dekker, Phys. Rev. B **65**, 115423 (2002).
[20] S. Berber, Y. K. Kwon, and D. Tomanek, Phys. Rev. Lett. **84**, 4613 (2000).
[21] Q. Zheng, G. Su, J. Wang, and H. Guo, Eur. Phys. J. B **25**, 233 (2002).
[22] P. Kim, L. Shi, A. Majumdar, and P. L. McEuen, Phys. Rev. Lett. **87**, 215502 (2001).
[23] T. Hertel, R. E. Walkup, and P. Avouris, Phys. Rev. B **58**, 13 870 (1998).
[24] A. Rochefort, P. Avouris, F. Lesage, and D. R. Salahub, Phys. Rev. B **60**, 13824 (1999).
[25] M. B. Nardelli and J. Bernholc, Phys. Rev. B **60**, R16 338 (1999).
[26] A. O. Gogolin, A. A. Nersesyan, and A. M. Tsvelik, *Bosonization and Strongly Correlated Systems* (Cambridge University Press, Cambridge, 1998).
[27] R. Egger and A. O. Gogolin, Eur. Phys. J. B **3**, 281 (1998).
[28] R. Egger, H. Grabert, A. Koutouza, H. Saleur, and F. Siano, Phys. Rev. Lett. **84**, 3682 (2000).
[29] Z. Yao, C. L. Kane, and C. Dekker, Phys. Rev. Lett. **84**, 2941 (2000).